PROCEEDINGS, 41st Workshop on Geothermal Reservoir Engineering
Stanford University, Stanford, California, February 22-24, 2016
SGP-TR-209

Operator-based Linearization for Modeling of Low-enthalpy Geothermal Processes

Mark Khait, Denis Voskov

Stevinweg 1, 2628 CN Delft

m.khait@tudelft.nl

Keywords: parametrization of physics, geothermal simulation, low enthalpy geothermal

ABSTRACT

Simulation of geothermal processes is based on the solution of strongly nonlinear governing equations describing flow of mass and energy in the subsurface. The solution of this problem requires a linearization of governing equations. Recently, a new approach based on the operator-based multi-linear representation of conservation equations was proposed for an isothermal flow and transport. The discretized version of conservation equations was transformed to the operator form where each term of the equation was represented as a product of two operators: one dependent on physical properties of fluids (e.g. density or viscosity) and another dependent on properties, altered in space (e.g. porosity or permeability). The first type of operators was parametrized in the physical space of the simulation problem at the pre-processing stage, or adaptively during the course of simulation. Next, multi-linear interpolation was applied for physics-based operators when the linearization of the second type of operators was performed in a conventional manner. In this work, the approach has been extended for the thermal processes. The operator-based parametrization was performed using temperature, pressure and composition. The performance and robustness of the method was tested against the conventional approach on low enthalpy models of geothermal reservoirs of practical interest.

1. INTRODUCTION

Modern development of geothermal resources requires numerical reservoir simulations. They are used to predict and compare the performance of different reservoir development schemes as well as to reduce uncertainties in parameters estimation. Growing computational power available in the high performance computing market spawned a higher demand for more complex, accurate and sizeable models. However, these complexities often challenge the performance of the simulation process. Examples include challenges due to computational grid complexity, as in Magnúsdóttir (2013), or large time steps in simulation, which was observed by Noy et al. (2012). Both space and time approximations introduce nonlinearity to the system of equations that need to be solved numerically.

One of the most important and challenging steps performed after the discretization stage is the linearization of a whole system of equations which involves an assembly of a Jacobian matrix. This step requires the determination of the derivatives of all the residual equations with respect to independent variables. The particular set of independent variables is defined by the nonlinear formulation of the particular simulation framework. Based on the formulation, all properties and their derivatives need to be determined with respect to nonlinear unknowns. Numerical derivatives provide flexibility in the implementation (see TOUGH2 by Pruess et al. 1999 for example), but usually lack the robustness (Vanden, 1996). Straightforward analytical derivations require fixing the nonlinear formulation and physical models used in computational framework and that often limits its flexibility (e.g. Geoquest, 2011 or CMG, 2012).

The development of Automatic Differentiation (AD) techniques provides both flexibility and robustness to the development of simulators. In reservoir simulation, the AD-based library (ADETL) was introduced first by Younis (2009), and significantly extended later by Zhou (2012). Using the capabilities of ADETL, an Automatic Differentiation General Purpose Research Simulator (ADGPRS) was developed by Voskov et al. (2009). ADGPRS is a unified reservoir simulation framework providing an extensive set of nonlinear formulations (Voskov, 2011; Voskov and Tchelepi, 2012; Zaydullin et al. 2012), flexible spatial discretization (Zhou et al., 2011), extended physics models (Iranshahr et al., 2013; Zaydullin et al., 2014; Garipov et al. 2014) and inverse capabilities (Kourounis et al. 2010; Volkov and Voskov, 2015). Recently, a geothermal formulation was developed in ADGPRS by Wong et al. (2015). In this study we also use ADGPRS for the implementation of a new nonlinear formulation and linearization approach.

The predecessor of the new linearization technique described in this work was the Compositional Space Parametrization (CSP) method proposed in Voskov and Tchelepi (2011) and fully developed by Zaydullin et al. (2012). In this approach, a complex thermodynamic phase behavior is described by a special set of nonlinear unknowns: pressure, phase fractions and tie-line parameters. All properties are defined in a discretized tie-simplex space, resulting in a piece-wise linear representation of a complex multicomponent thermodynamics based on nonlinear unknowns. This technique allows expensive phase behavior computations in the course of simulation to be minimized.

Inspired by CSP method, a new linearization approach was recently introduced by Voskov (2016). In conventional reservoir simulation, the discretization of the governing PDEs is always performed approximately introducing time and space truncation errors. At the same time, all physical properties are usually introduced in a very precise manner based on results of lab experiments or known correlations. Partially due to this reason, the nonlinear solver often requires a lot of iterations in order to resolve all challenging features introduced by the precise physics of the process.

The new approach suggests a different way of linearization. Each term in the discretized conservation equations is represented by a product of two operators: state- and space-dependent. The state-dependent operator describes a part of the term dependent on rock and fluid physical properties. The space-dependent operator represents a spatially altered part of the properties. The state-dependent operators are parametrized over the physical space of simulation problem at a pre-processing stage. In the course of simulation, the state-dependent operators are calculated based on a multilinear interpolation in a multidimensional space of nonlinear parameters. The space-dependent operator is calculated in conventional manner.

Here we present an extension of this approach to thermal systems where the discrete version of the energy equation is linearized based on state-dependent and space-dependent operators. The new approach demonstrates better nonlinear performance of simulations with coarser representation of physics where an approximation error is controlled by the resolution of interpolation tables. Several directions for the extension of this approach are discussed in the conclusion.

2. MODELING APPROACH

2.1 Governing Equations for Thermal Compositional Problem

This section contains a description of thermal multiphase compositional problem. This problem can be described by n_c equations of mass conservation and one energy equation:

$$\frac{\partial}{\partial t}\left(\phi \sum_{j=1}^{n_p} x_{cj}\rho_j s_j\right) + \mathrm{div}\sum_{j=1}^{n_p} x_{cj}\rho_j u_j + \sum_{j=1}^{n_p} x_{cj}\rho_j \tilde{q}_j = 0, \qquad c = 1, \dots, n_c \tag{1}$$

$$\frac{\partial}{\partial t}\left(\phi \sum_{j=1}^{n_p} \rho_j s_j U_j + (1-\phi)U_r\right) + \mathrm{div}\sum_{j=1}^{n_p} h_j\rho_j \overrightarrow{u_j} + \mathrm{div}(\kappa\nabla T) + \sum_{j=1}^{n_p} h_j\rho_j \tilde{q}_j = 0. \tag{2}$$

All terms in the system above can be introduces as functions of spatial coordinate ξ and/or physical state ω:

- $\phi(\xi, \omega)$ – porosity,
- $x_{cj}(\omega)$ – the mole fraction of component c in phase j,
- $s_j(\omega)$ – phase saturations,
- $\rho_j(\omega)$ – phase molar density,
- $\overrightarrow{u_j}(\xi, \omega)$ – phase velocity,
- $\mathrm{U}_j(\xi)$ – phase internal energy,
- $\mathrm{U}_r(\xi, \omega)$ – rock internal energy,
- $h_j(\xi)$ – phase enthalpy,
- $\kappa(\xi, \omega)$ – thermal conduction.

The only exception is the well phase rate per unit volume $\tilde{q}_j$ that could be written as $\tilde{q}_j = \tilde{q}_j(\xi, \omega, u)$, where u is the well control variable. To simplify the description further, we will consider the initial porosity ϕ_0 as a pseudo-physical state variable, so $\phi = f(\omega)$. This is a key change to the original approach by Voskov (2016). Another simplification, based on assumption that rock internal energy and thermal conduction are spatially homogeneous, is:

$$\mathrm{U}_r = f(\omega), \qquad \kappa = f(\omega) \tag{3}$$

Darcy's law is used to define the flow velocity:

$$\overrightarrow{u_j} = -\left(K\frac{k_{rj}}{\mu_j}\left(\nabla p_j - \gamma_j \nabla D\right)\right), \qquad j = 1, \dots, n_p, \tag{4}$$

where

- $K(\xi)$ – permeability tensor,
- $k_{rj}(\omega)$ – relative permeability,
- $\mu_j(\omega)$ – phase viscosity,
- $p_j(\omega)$ – pressure in phase j,
- $\gamma_j(\omega)$ – gravity vector,
- $D(\xi)$ – depth (backward oriented).

Next we apply a finite-volume discretization on a general unstructured mesh and backward Euler approximation in time:

$$V\left[\left(\phi\sum_{j=1}^{n_p} x_{cj}\rho_j s_j\right)^{n+1} - \left(\phi\sum_{j=1}^{n_p} x_{cj}\rho_j s_j\right)^{n}\right] - \Delta t\sum_l\left(\sum_{j=1}^{n_p} x_{cj}^l\rho_j^l\Gamma_j^l\Delta\psi^l\right) + \Delta t\sum_{j=1}^{n_p}\rho_p x_{cj}q_j = 0, \qquad c = 1,\dots,n_c \quad (5)$$

$$V\left[\left(\phi\sum_{j=1}^{n_p}\rho_j s_j U_j + (1-\phi)U_r\right)^{n+1} - \left(\phi\sum_{j=1}^{n_p}\rho_j s_j U_j + (1-\phi)U_r\right)^{n}\right]$$

$$-\Delta t\sum_l\left(\sum_{j=1}^{n_p} h_j^l\rho_j^l\Gamma_j^l\Delta\psi^l + \Gamma_c^l\Delta T^l\right) + \Delta t\sum_{j=1}^{n_p} h_j\rho_j q_j = 0 \quad (6)$$

where V is a control volume and $q_j = \tilde{q}_j V$ is a source of phase j. In the equations above we have neglected capillarity, gravity and applied a Two-Point Flux Approximation (TPFA) with an upstream weighting. Based on these simplifications, $\Delta\psi^l$ becomes a simple difference in pressures between blocks connected via interface l, while ΔT^l is a temperature difference between those blocks; $\Gamma_j^l = \Gamma^l k_{rj}^l/\mu_j^l$ is a phase transmissibility, where Γ^l is a constant geometrical part of transmissibility (which involves permeability and geometry of control volume). Finally $\Gamma_c^l = \Gamma^l\kappa$ is a thermal transmissibility.

2.2 Operator Form of Conservation Equations

Next, according to the original proposed approach (Voskov, 2016), we rewrite equations (5) and (6) representing each term as a product of state-dependent and space-dependent operators. The mass conservation equation reads:

$$a(\xi)\big(\alpha_c(\omega) - \alpha_c(\omega_n)\big) + \sum_l b(\xi,\omega)\beta_c(\omega) + \theta_c(\xi,\omega,u) = 0, \qquad c = 1,\dots,n_c, \quad (7)$$

where

$$a(\xi) = V(\xi),$$

$$\alpha_c(\omega) = \phi_0\left(1 + c_r\big(p - p_{ref}\big)\right)\textstyle\sum_{j=1}^{n_p} x_{cj}\rho_j s_j,$$

$$b(\xi,\omega) = \Delta t\Gamma^l(\xi)(p^b - p^a),$$

$$\beta_c(\omega) = \textstyle\sum_{j=1}^{n_p} x_{cj}^l\rho_j^l\frac{k_{rj}^l}{\mu_j^l},$$

$$\theta_c(\xi,\omega,u) = \Delta t\textstyle\sum_{j=1}^{n_p} x_{cj}\rho_j q_j(\xi,\omega,u).$$

Here

- ω, ω_n – state variables on the current and previous timestep respectively,
- c_r – rock compressibility,
- p^a, p^b – pressures in blocks a and b connected through interface l,
- $\gamma_j(\omega)$ – gravity vector.

The energy conservation equation can be presented as:

$$a_e(\xi)\big(\alpha_e(\omega) - \alpha_e(\omega_n)\big) + \sum_l b_e(\xi,\omega)\beta_e(\omega) + \sum_l c_e(\xi,\omega)\gamma_e(\omega) + \theta_e(\xi,\omega,u) = 0, \quad (8)$$

where

$$a_e(\xi) = V(\xi),$$

$$\alpha_e(\omega) = \phi_0\big(1 + c_r(p - p_{ref})\big)\big(\textstyle\sum_{j=1}^{n_p}\rho_j s_j U_j - U_r\big) + U_r,$$

$$b_e(\xi,\omega) = b_m(\xi,\omega),$$

$$\beta_e(\omega) = \textstyle\sum_{j=1}^{n_p} h_j^l\rho_j^l\frac{k_{rj}^l}{\mu_j^l},$$

$$c_e(\xi) = \Gamma^l(T^b - T^a),$$

$$\gamma_e(\omega) = \phi_0\big(1 + c_r(p - p_{ref})\big)\big(\sum_{j=1}^{n_p} s_j\lambda_j - \lambda_r\big) + \lambda_r,$$

$$\theta_e(\xi, \omega, u) = \Delta t \sum_{j=1}^{n_p} h_j\rho_j q_j(\xi, \omega, u).$$

Here T^a, T^b correspond to temperatures in grid blocks, connected by the interface l. These transformations identify and distinguish the physical state dependent operators $(\alpha_c, \beta_c, \alpha_e, \beta_e, \gamma_e)$ in both the mass (5) and the energy (6) conservation equations. The only exception is the source/sink term which can also be processed in a similar manner based on state, space and additional well control variables. We leave this for the future research.

2.3 Nonlinear Formulation and Conventional Linearization Approach

Equations (5) and (6) are approximated in time using a Fully Implicit Method (FIM). This suggests that convective flux terms $x_{cj}^l\rho_j^l\Gamma_j^l\Delta\psi^l$ for mass and $h_j^l\rho_j^l\Gamma_j^l\Delta\psi^l$ for energy equation as well as the conductive flux $\Gamma_c^l\Delta T^l$ have to be chosen based on values of nonlinear unknowns at the current time step, which introduce nonlinearity to the system. Also, the closure assumption on instantaneous thermodynamic equilibrium further amplifies nonlinearities.

Among the different nonlinear formulations we have chosen an overall molar formulation (Collins et al. 1992). In this formulation, thermodynamic equilibrium is required at every nonlinear iteration. Hence, the following system has to be solved at any grid block contained a multiphase (n_p) multicomponent (n_c) mixture:

$$F_c = z_c - \sum_{j=1}^{n_p} \nu_j x_{cj} = 0, \tag{9}$$

$$F_{c+n_c} = f_{c1}(p, T, x_1) - f_{cj}\big(p, T, x_j\big) = 0, \tag{10}$$

$$F_{j+n_c\times n_p} = \sum_{c=1}^{n_c} \big(x_{c1} - x_{cj}\big) = 0, \tag{11}$$

$$F_{n_p+n_c\times n_p} = \sum_{j=1}^{n_p} \nu_j - 1 = 0. \tag{12}$$

This procedure is called multiphase flash. Here $z_c = \sum_{j=1}^{n_p} x_{cj}\rho_j s_j / \sum_{j=1}^{n_p} \rho_j s_j$ is the overall composition, $f_{cj}(p, T, x_{cj})$ is the fugacity of component c in phase j and $\nu_j = \rho_j s_j / \sum_j \rho_j s_j$ is mass fraction of the phase. The multiphase flash solution provides the values of x_{cj} and ν_j. In the molar formulation, the unknowns are p, z_c and T (or h). The physical state ω is completely defined by these variables but, as mentioned above, we have introduced a pseudo-state variable ϕ_0 to the set. This step not only allows us to reduce the number of state-dependent operators but also provides a way to extend the compositional model to systems with precipitation and dissolution of solid phase(s). As soon as we obtain the solution of multiphase flash, we can determine all derivatives with respect to nonlinear unknowns using the inverse theorem (see Voskov and Tchelepi, 2012 for details).

The conventional linearization approach is based on the Newton-Raphson method, which solves on each nonlinear iteration a linear system of equations in the following form:

$$J(\omega^k)(\omega^{k+1} - \omega^k) + r(\omega^k) = 0, \tag{13}$$

where J is the Jacobian defined at a nonlinear iteration k. The conventional approach assumes a numerical representation of properties and their derivatives with respect to nonlinear unknowns. This may demand either table interpolation (for properties such as relative permeabilities) or solution of a highly nonlinear system (9-12) (for properties defined by an Equation of State) in combination with chain rule and inverse theorem. As a result, the nonlinear solver has to resolve all features of property descriptions, which are sometimes unimportant but might be quite challenging due to the numerical nature and/or uncertainties in property evaluation.

2.4 Interpolation-Based Linearization Approach

In this approach we simplify the description of fluid and rock properties based on an approximate representation of operators $\alpha_c, \beta_c, \alpha_e, \beta_e$ and γ_e within the parameter-space of a simulation problem. In further derivations we limit the description by two-component system that is sufficient for geothermal applications. In binary systems, we only have three independent variables in the case of overall molar formulation: pressure p, temperature T and one independent overall composition z. The pressure and temperature ranges are defined by initial and production/injection conditions at wells, while the overall composition is naturally limited by the interval [0,1]. As mentioned above, we add the initial porosity ϕ_0 as a pseudo-physical state variable with the corresponding range [0,1].

Next we parameterize the interval of each state variable using the same number of uniformly distributed points in the intervals of parameters. This results in a set of vectors p^m, t^m, z^m and ${\phi_0}^m$ which can be interpreted as a discrete representation of physical space

in the simulation. At the pre-processing stage we evaluate operators $\alpha_c, \beta_c, \alpha_e, \beta_e$ and γ_e at every point of discrete parameter space $\{p^m, t^m, z^m, {\phi_0}^m\}$ and store them in four-dimensional tables ${\alpha_c}^m, {\alpha_e}^m$ and three-dimesional tables ${\beta_c}^m, {\beta_e}^m, {\gamma_e}^m$ (since β_c and β_e are independent of ϕ_0 and γ_e is independent of T). During the course of simulation we interpolate state-dependent operators using created tables for each grid block. This provides a continuous description based on the interpolation operator whose accuracy is controlled by the resolution of discretization in the parameter space.

This representation simplifies significantly the implementation of any complex simulation frameworks. Instead of keeping track of each property and its derivatives with respect to nonlinear unknowns, we can construct an algebraic system of equations with abstract algebraic operators representing the complex physics. The performance of this formulation benefits from the fact that all the expensive evaluations can be done at the pre-processing stage in the limited number of supporting points and are not required in the course of simulation. Finally, the performance of the nonlinear solver can be improved since the Jacobian is constructed based on a combination of piece-wise linear operators directly dependent on nonlinear unknowns.

3. NUMERICAL RESULTS

In this section we introduce numerical results of simulations based on the described approach. First we present a three-dimensional heterogeneous model describing a realistic reservoir for low-enthalpy geothermal operations. We show the comparison between simulation using the conventional geothermal formulation in ADGPRS (Wong et al. 2015) and the COMSOL simulation platform (COMSOL, 2015). Next, using the same model, we present a convergence study of the operator-based linearization for the one-component geothermal model based on different resolutions of parameterized tables. Finally, a similar convergence analysis will be performed for a geothermal system with natural gas co-production.

3.1 Three-dimensional Realistic Heterogeneous Geothermal Reservoir

Here we present results of a geothermal simulation based on a realistic geological model has been made by Willems et al. (2016). This model is one of the realizations of sedimentological simulation for the Nieuwerkerk sedimentary formation in the West Netherlands Basin. These models have been generated for an investigation of a doublet (a pair of injection and production wells) performance in low-enthalpy geothermal systems. Reservoir dimensions are 1km x 2 km x 20 m, the discretized model contains 50x100x20 grid blocks. Both wells are placed in the middle of model, along the long side with spacing of 1 km, see Fig.1. The paleo flow is located along the longer side of reservoir with the porosity distributed within the range [0.16, 0.36] and permeability distributed within the range [6, 3360]. The boundary conditions on the short sides of the reservoir are set to a constant initial pressure whereas the boundary conditions at the other two sides are set to no flow.

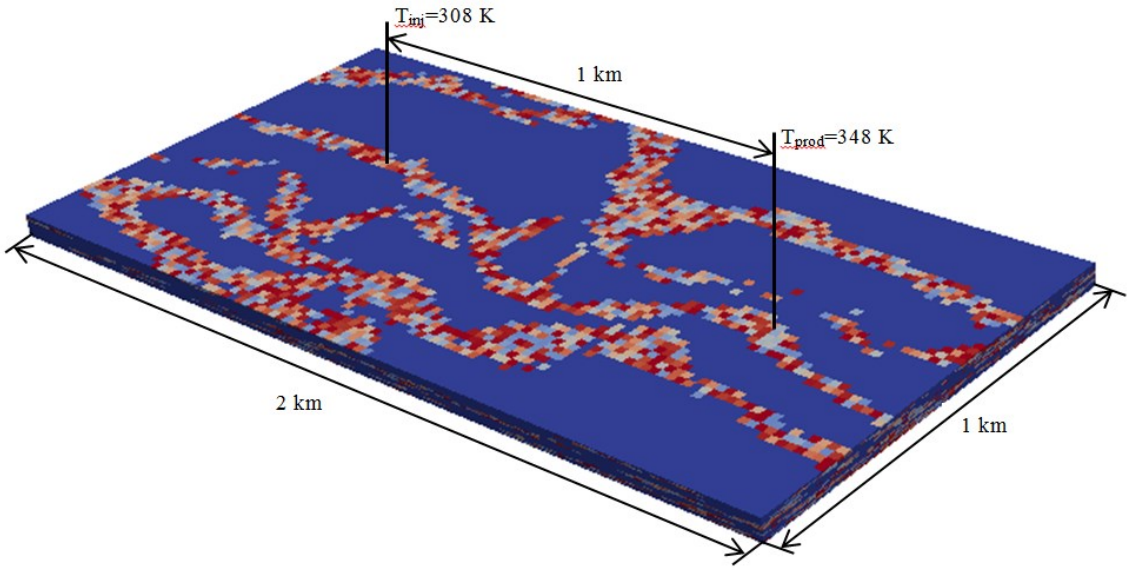

Figure 1: Realistic heterogeneous geothermal reservoir

Both wells operate under a constant water rate control q = 2400 m^3/day. The production well consumes energy from the reservoir, producing hot water at a reservoir temperature T_{prod} = 348 K. The injection well returns a cold water to the reservoir at T_{inj} = 308 K, forcing a cold front propagation to the production well. Both wells are perforated through all layers of the model. The two energy transfer mechanisms are involved in this process: fluid flow and heat conduction. When the cold front arrives at the production well, temperature drops below a certain limit (338 K in this study) and the so-called doublet lifetime is reached.

To verify the conventional geothermal formulation in the ADGPRS framework, we compare our simulation results with the original COMSOL model described in Willems et al (2016). Unlike ADGPRS which is based on a finite-volume discretization, the COMSOL utilizes a standard finite-element discretization which is not conservative. In Fig.2 we show the comparison between the temperatures at the production well for both simulations.

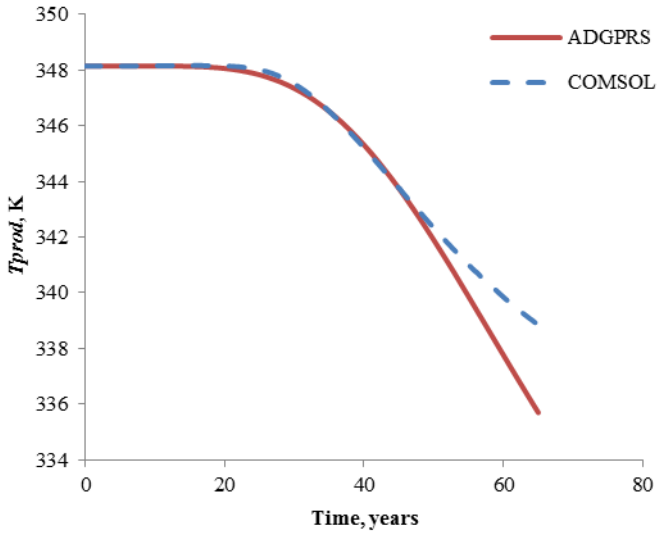

Figure 2: Comparison between COMSOL and ADGPRS realistic heterogeneous reservoir simulation results

As you can see, the ADGPRS and COMSOL results are very similar until the time around 50 years when the temperature reduction is already quite significant. These differences can be explained by the differences in the spatial discretization. We also believe that the temperature reduction, caused by a cold front of water injected at $T = 308$ K approaching the production well, looks more realistic in the ADGPRS simulation results.

3.2 One-Component Geothermal Model

3.2.1 Convergence of Operator-based Linearization

In this section we compare the results of simulation for operator-based linearization performed at different resolutions of interpolation tables and the reference solution based on the conventional linearization method. The reduced version of the operator-based linearization approach for one-component one-phase system is described in Appendix A.

We use a simplified variant of the original test case with uniformly distributed thermal properties of rock while rock permeabilities and porosities remain heterogeneous. Both wells work at the same rate control q = 2400 m^3/day. Each simulation was performed with a different number of points in the interpolation table which, for simplicity, was equal for all of the unknowns (p, t and φ) while values were uniformly distributed within the range between p_{min}=150 bars and p_{max}=250 bars for pressure, T_{min}=300 K and T_{max}=350 K for temperature, and between 0 and 1 for porosity. In order to estimate the error between the reference solution and the solution obtained with operator-based linearization, the following error estimation was introduced:

$$\mathrm{E} = \frac{\sum_{i=0}^{n} \left| {x^i}_{interp} - {x^i}_{ref} \right|}{n \left(\max\left({x^0}_{ref}, \ldots, {x^n}_{ref}\right) - \min\left({x^0}_{ref}, \ldots, {x^n}_{ref}\right) \right)} \tag{14}$$

Here n is a number of blocks in the model, x^i is a particular solution value at grid block i. This error was determined at the end of simulation (65 years) for both temperature and pressure variables. The results of comparison are presented in Table 1. The number of points used for interpolation operators is shown in the first column. The second column contains the number of nonlinear iterations. The third and fourth columns represent the error in the temperature and pressure solution respectively.

Table 1: Results of 3D homogeneous simulation

Resolution	Newton iters.	$E_{T,\%}$	$E_{p,\%}$
Standard	193	-	-
64	193	0.0952	0.0025
32	192	0.0952	0.0026
16	194	0.0955	0.0038
8	197	0.0960	0.0067
4	201	0.1040	0.0363
2	194	0.1385	0.1984

From Table 1, the results based on any parameterization approach show relatively small error. That is because all interpolated properties have substantially linear behavior with respect to the nonlinear unknowns. It seems sufficient in this model to perform the operator-based linearization using the coarsest resolution (2 points). This conclusion is also supported by the comparison of the production temperatures and temperature distribution, as shown in Fig.3 and Fig.4 respectively. Fig.3 demonstrates almost complete match between reference and parameterization approach based solutions. As you can see from Fig.4 the cold front propagates over the middle layer of reservoir after 15, 30 and 45 years of simulation. No noticeable differences between the conventional and new linearization approaches can be detected.

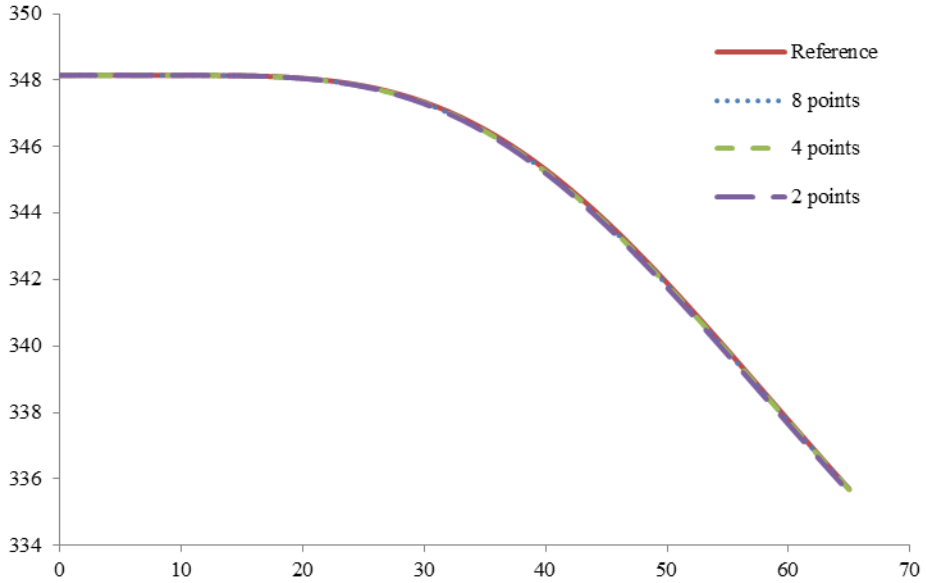

Figure 3: Comparison of temperatures at production well based on different linearization approaches

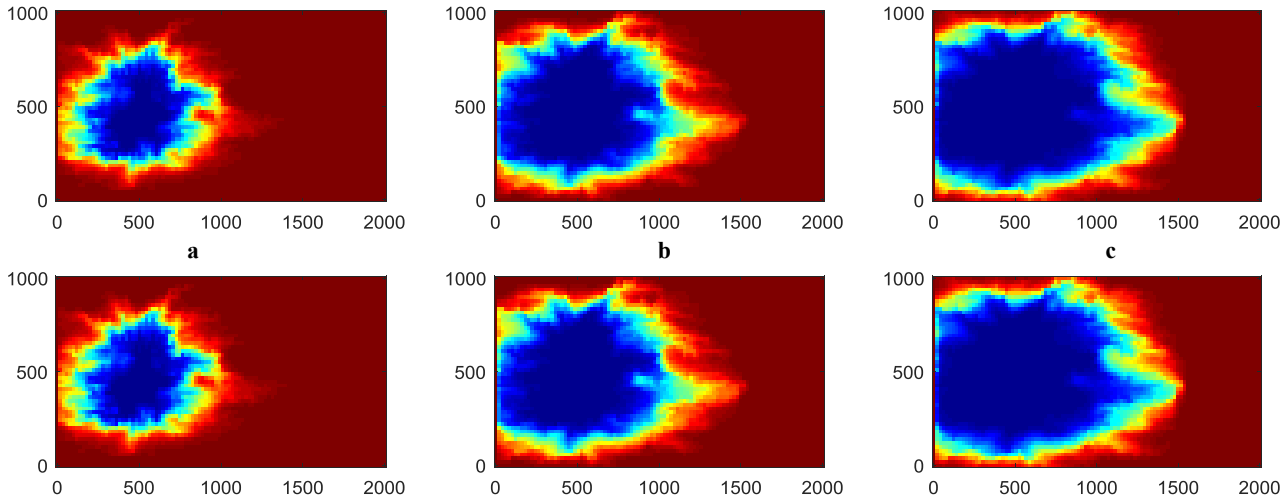

Figure 4: Cold front after 15 (a), 30 (b) and 45 (c) years for the conventional (upper) and the proposed (lower) linearization approaches

3.2.2 An Analysis of Linearization Operators

In Fig.5 we present the most nonlinear operators used in the proposed linearization approach. All of them are built based on the 64-point interpolation tables in parameter space. These operators correspond to the linearization of mass accumulation α_m and flux β_m terms in the mass equation and energy accumulation α_e and conduction γ_e in the energy equation (see Appendix A for detailed description). They are represented by isosurfaces in pressure, temperature and porosity parameter space. As expected, all of the operators behave quite linearly in parameter space that explains why the results of simulation with the coarsest operator are acceptable.

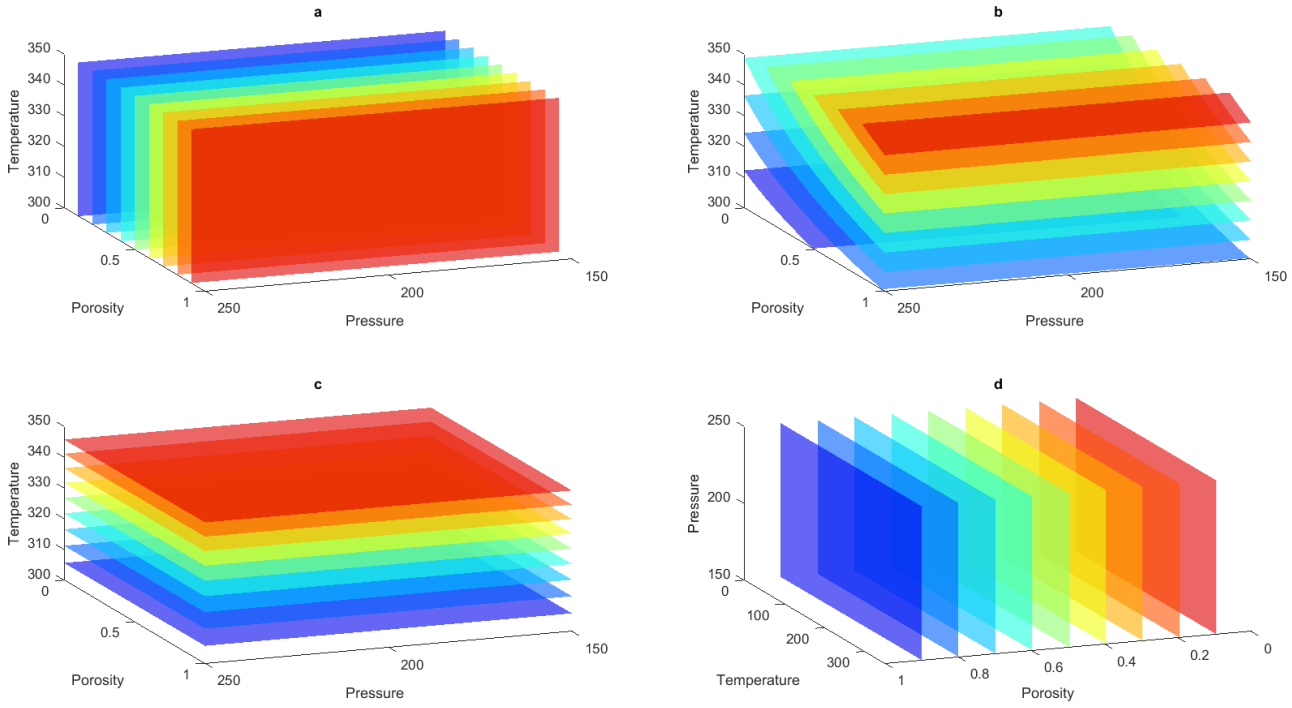

Figure 5: Physics-based operators of mass accumulation (a), energy accumulation (b), mass flux (c) and energy conduction (d) terms

3.3 Two-Component Geothermal Model

3.3.1 Convergence of Operator-based Linearization

Here we demonstrate geothermal simulation with gas co-production using the same three-dimensional reservoir. The injection well injects cold water at T^w=308K and controlled by a water rate q^w = 1200 m^3/day. The initial reservoir composition of the gas component (methane) is z_1 = 0.1 with initial pressure p=100 bars and initial temperature T=348 K. The production well is controlled by a bottom hole pressure p^w=70 bars. The simulation period is 15 years.

We performed a set of simulations with 6 different interpolation table resolutions and compared solutions with the reference model based on the conventional approach. For parameterization we used a uniformly distributed points between p_{min}=60 bars and p_{max}=150 bars for pressure, T_{min}=300 K and T_{max}=360 K for temperature, z_{min}=0 and z_{max}=0.2 for composition and finally between 0 and 1 for porosity. The results can be seen in Table 2. Columns 1-4 are same as in Table 1, while the fifth column shows the error in composition.

Table 2: Results of 3D two-phase simulation

Resolution	Newton iters.	$E_{T,\%}$	$E_{p,\%}$	$E_{z,\%}$
Standard	867	-	-	-
64	748	0.1853	0.0448	0.2126
32	695	0.1783	0.1364	0.5957
16	629	0.3497	0.2427	1.1073
8	626	0.6286	0.4012	1.5354
4	641	1.1512	0.8092	2.038
2	498	3.046	1.0304	2.7999

The two-component two-phase geothermal model is more challenging for the operator-based linearization approach in comparison to the previous case. However, the error of the operator-based linearization drops significantly with the resolution of interpolation tables. Production temperatures for the reference solution and solutions based on linearization operator are shown in Fig.6. Here you can see that the simulation based on the coarsest table introduces non-physical initial grow of temperature due to a very coarse approximation of operators involved in the energy equation. However, this behavior is quickly stabilized for the cases with a higher resolution. The comparison of thermal front is shown in Fig.7. Here you can see the reference solution (upper figures) and the solution based on the operator-based linearization with 2 points only and that no significant difference similar to one shown in Fig. 6 can be observed.

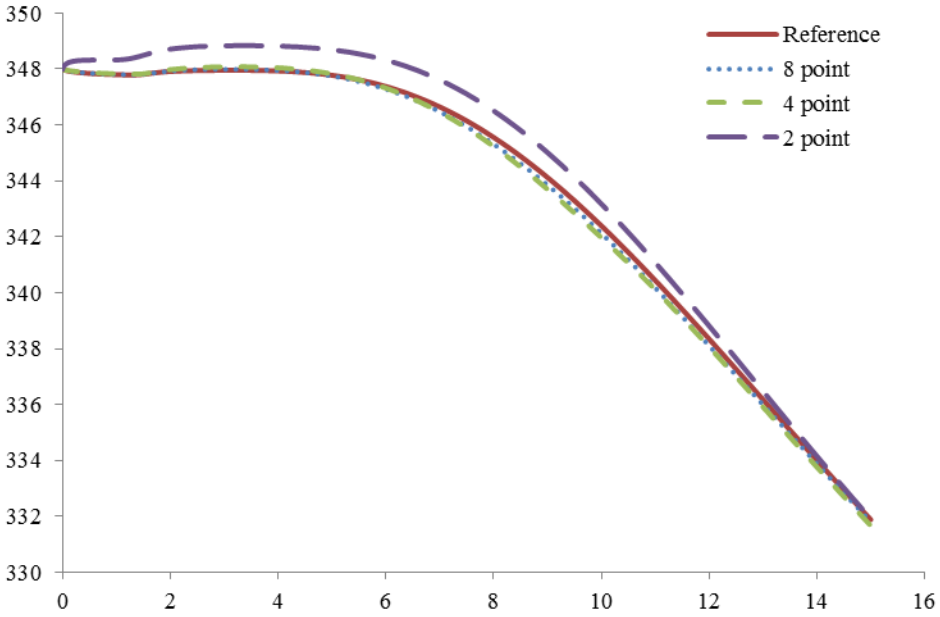

Figure 6: Comparison of temperatures at production well based on different linearization approaches

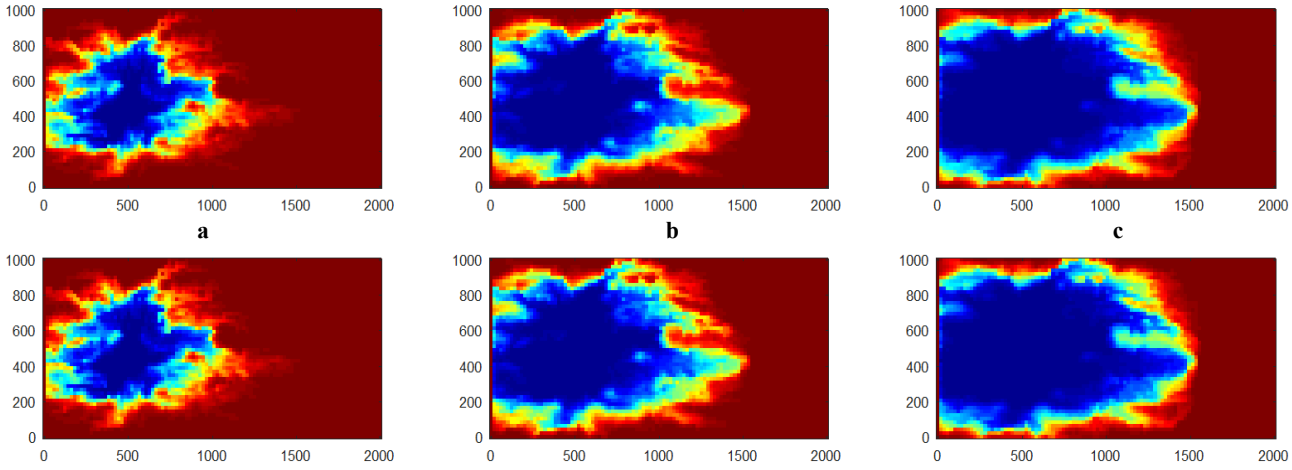

Figure 7: Cold front after 15 (a), 30 (b) and 45 (c) years for the conventional (upper) and the proposed (lower) linearization approaches

3.3.2 The Analysis of Linearization Operators

In Fig.8 we plot 3D isosurfaces to describe the most nonlinear operators in the case of two-phase geothermal model. These operators correspond to the linearization of mass accumulation α_1 and flux β_1 terms for gas component in the mass equation and energy accumulation α_e and flux β_e in the energy equation. All of the operators are built based on the 64-point interpolation table. They are shown as functions of pressure, temperature and composition at the constant $\varphi = 0.2$. Unlike the pure geothermal case, all operators are highly nonlinear as functions of all state variables.

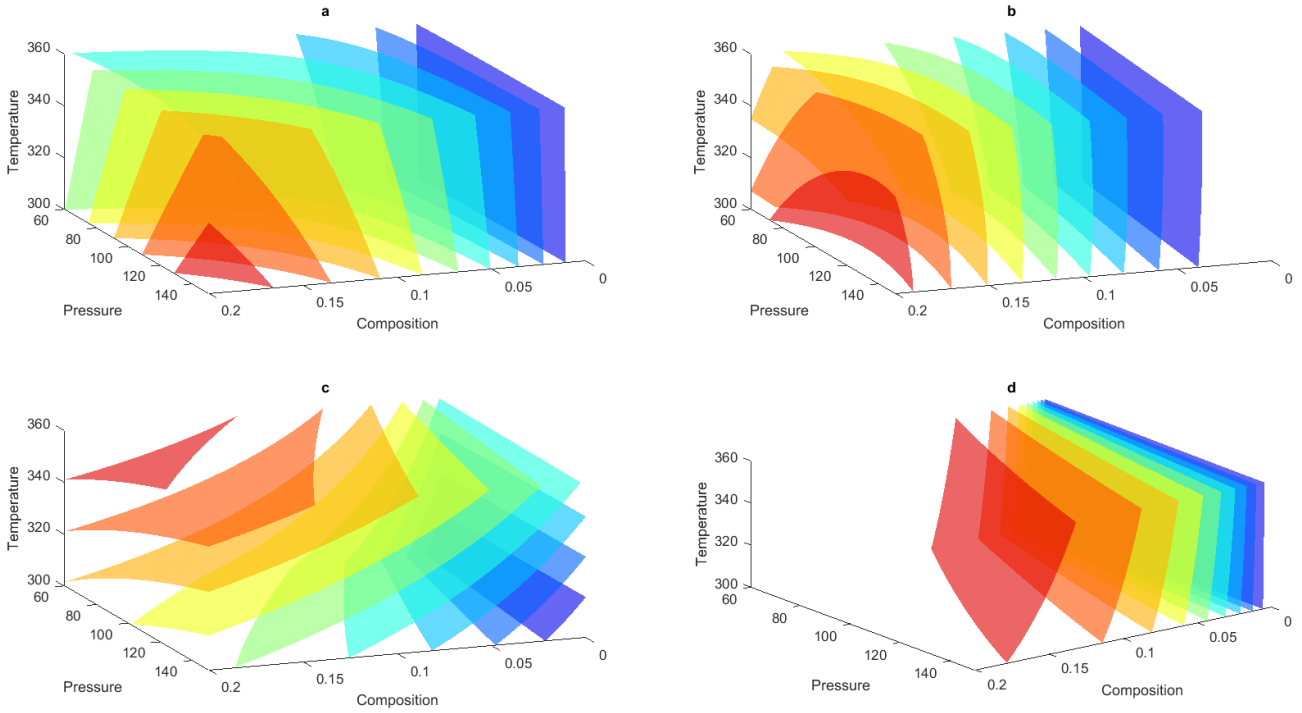

Figure 8: Physics-based operators of mass accumulation for gas component (a), energy accumulation (b), mass flux for gas component (c) and energy flux (d) terms

4. CONCLUSION

In this paper we demonstrated the applicability of an operator-based linearization approach to the simulation of thermal multi-component multiphase flow in porous media. Both mass and energy conservation equations were transformed to operator form where each term was represented as a product of state-dependent and space-dependent operators. During the pre-processing stage, all state-dependent operators were discretized in the parameter space of simulation problems and introduced as a set of interpolation tables. In the course of simulation, these operators were updated based on multilinear interpolation while the rest of the equation terms were computed using the conventional approach. The operator-based linearization was applied to a geothermal system with gas co-production where pressure, temperature, composition and initial porosity were used as state parameters. The addition of porosity to the state variables helps to reduce the number of state-dependent operators. A similar mechanism can be used to handle the changes in mass of solid phase(s) due to precipitation and dissolution processes.

We used a realistic reservoir model of low-enthalpy geothermal doublet to test the approach. Simulation results showed that proposed approach can reproduce the reference solution results quite accurately with a reasonable resolution of interpolation tables. For a single component low-enthalpy geothermal model, an extremely coarse resolution of interpolation tables was able to handle all governing nonlinearities and matched the reference solution based on full physics almost precisely. For a two-component geothermal model with natural gas co-production, the required resolution of interpolation tables is higher. This happened due to the highly-nonlinear nature of linearization operators in case of two-component two-phase system.

The extended approach described in this paper inherits all the benefits of the original approach proposed for isothermal system. The method substantially simplifies the assembly of the residual and Jacobian. At the same time, the operator-based version of the original problem could be seen as a proxy model where the accuracy of the nonlinear representation of the physics can be balanced with the performance of nonlinear solver. Here we used the most straightforward approach and defined the parameter space of the problem explicitly in a uniform fashion. However, for a general purpose simulation, an adaptive parametrization in parameter space looks more attractive both in terms of efficiency and memory management. The combination of the adaptive parametrization and coarsening of tables based on a simple error estimator provides an excellent opportunity for nonlinear analysis. The refined parametrization in the physical space would then indicate the most nonlinear behavior of the governing equations and open possibility to construct an advanced nonlinear solver based on trust-region technique.

REFERENCES

CMG: STARS user's guide (2009)

Collins, D., Nghiem, L., Li, Y.K., Grabenstetter, J.: Efficient approach to adaptive-implicit compositional simulation with an equation of state. *SPEJ* 7(2), 259–264 (1992)

COMSOL: COMSOL Multiphysics Reference Manual, 5.1 (2015)

Garipov, T.T., Karimi-Fard, M., Tchelepi, H.A.: Fully coupled flow and geomechanics model for fractured porous media. *In: 48th US Rock Mechanics / Geomechanics Symposium* 2014 (2014)

Geoquest: Eclipse Technical Description 2011.2. Schlumberger (2011).

Iranshahr, A., Voskov, D.V., Tchelepi, H.A.: Tie-simplex based compositional space parameterization: Continuity and generalization to multiphase systems, *AIChE Journal*, 59, 1684-1701 (2013)

Kourounis D., Voskov D., Aziz K., Adjoint Methods for Multicomponent Flow Simulation, *Proceedings*, 12th European Conference on the Mathematics of Oil Recovery, Oxford, United Kingdom, (2010)

Magnúsdóttir, L.: Fracture Characterization in Geothermal Reservoirs using Time-Lapse Electric Potential Data, *Dissertation*, Stanford University, CA (2013).

Noy, D. J., Holloway, S. Chadwick, R.A., Williams, J.D.O., Hannis, S. A. and Lahann R.W.: "Modelling large-scale carbon dioxide injection into the Bunter Sandstone in the UK Southern North Sea, *International Journal of Greenhouse Gas Control,*9: 220-233 (2012).

Pruess, K., Oldenburg, C. M., and Moridis, G. J.: TOUGH2 User's Guide Version 2 (1999).

Vanden, K. J., and Orkwis, P. D.: Comparison of numerical and analytical Jacobians. *AIAA* journal 34(6), 1125-1129 (1996).

Volkov, O., Voskov, D.: Effect of time stepping strategy on adjoint-based production optimization. *Computational Geosciences* pp. 1–16 (2015).

Voskov D., Tchelepi H., Younis R.: General nonlinear solution strategies for multi-phase multi-component EoS based simulation, *SPE 118996, RSS*, Woodland, TX, February (2009)

Voskov, D.V.: An extended natural variable formulation for compositional simulation based on tie-line parameterization, *Transport in Porous Media*, 86 (2011)

Voskov, D.V., Tchelepi, H.A.: Compositional nonlinear solver based on trust regions of the flux function along key tie-lines. *Proceedings*, SPE Reservoir Simulation Symposium (2011)

Voskov, D. V., and Tchelepi, H. A.: Comparison of nonlinear formulations for two-phase multi-component EoS based simulation. *Journal of Petroleum Science and Engineering*, 82, 101-111 (2012).

Voskov, D. V.: Operator-based multilinear formulation for modeling of multiphase multi-component flow and transport, *Computational Geosciences,* 11 p. (submitted) (2016)

Willems, C.J.L., T. Goense; H.M. Nick; D.F. Bruhn.: The relation between well spacing and Net Present Value in fluvial Hot Sedimentary Aquifers; a West Netherlands Basin case study, *Proceedings*, 41st Workshop on Geothermal Reservoir Engineering, Stanford University, Stanford, CA (2016)

Wong, Z.Y., Horne, R., Voskov, D.: A Geothermal Reservoir Simulator in AD-GPRS, *Proceedings* World Geothermal Congress (2015)

Younis, R.M.: Advances in Modern Computational Methods for Nonlinear Problems; A Generic Efficient Automatic Differentiation Framework, and Nonlinear Solvers that Converge All The Time. PhD thesis, Stanford University (2009).

Zaydullin, R., Voskov, D.V., Tchelepi, H.A.: Nonlinear formulation based on an equation-of-state (eos) free method for compositional flow simulation. *SPEJ*, DOI: 10.2118/146989-PA (2012)

Zaydullin, R., Voskov, D., James, S., Lucia, A.: Fully compositional and thermal reservoir simulation. *Computers and Chemical Engineering* 63, 51 – 65 (2014)

Zhou, Y., Tchelepi H.A., Mallison B.T.: Automatic differentiation framework for compositional simulation on unstructured grids with multi-point discretization schemes. In *SPE Reservoir Simulation Symposium*. SPE 141592, (2011).

Zhou, Y.: Parallel general-purpose reservoir simulation with coupled reservoir models and multisegment wells. *Dissertation*. Stanford University, (2012a).

Zhou, Y.: ADETL User Manual, (2012b).

APPENDIX A. LOW-ETHALPY GEOTHERMAL REDUCTION

The standard geothermal formulation assumes only a water (brine) component and only one liquid phase. The discretized conservation equations (5-6) can be reduced to:

$$V((\phi\rho)^{n+1} - (\phi\rho^n)) - \Delta t \sum_l \left(\frac{\rho^l \Gamma^l \Delta\psi^l}{\mu^l}\right) + \Delta t \rho q = 0,$$

$$V((\phi\rho U_w + (1-\phi)U_r)^{n+1} - (\phi\rho U_w + (1-\phi)U_r)^n)) - \Delta t \sum_l \Gamma^l \left(\frac{h\rho^l \Delta\psi^l}{\mu^l} + \kappa^l \Delta T^l \right) + \Delta t h \rho q = 0,$$

where

- ρ – water density,
- μ – water viscosity,
- h – water enthalpy,
- q – source of water,
- U_w – water internal energy.

After the operator-based approach is applied, the equations read

$$a_m(\xi)\big(\alpha_m(\omega) - \alpha_m(\omega_n)\big) + \sum_l b_m(\xi,\omega)\beta_m(\omega) + \theta_m(\xi,\omega,u) = 0,$$

$$a_e(\xi)(\alpha_e(\omega) - \alpha_e(\omega_n)) + \sum_l b_e(\xi,\omega)\beta_e(\omega) + \sum_l c_e(\xi,\omega)\gamma_e(\omega) + \theta_e(\xi,\omega,u) = 0.$$

Here

$$a_m(\xi) = V(\xi),$$

$$\alpha_m(\omega) = \phi_0\big(1 + c_r(p - p_{ref})\big)\rho,$$

$$b_m(\xi,\omega) = \Delta t \Gamma^l(\xi)(p^b - p^a),$$

$$\beta_m(\omega) = \frac{\rho^l}{\mu^l},$$

$$\theta_m(\xi,\omega,u) = \Delta t \rho q(\xi,\omega,u).$$

$$a_e(\xi) = V(\xi),$$

$$\alpha_e(\omega) = \phi_0\big(1 + c_r(p - p_{ref})\big)(\rho U_w - U_r) + U_r,\ U_w = h - \frac{P}{\rho}$$

$$b_e(\xi,\omega) = b_m(\xi,\omega),$$

$$\beta_e(\omega) = h\beta_m(\omega),$$

$$c_e(\xi) = \Gamma^l(T^b - T^a),$$

$$\gamma_e(\omega) = \phi_0\big(1 + c_r(p - p_{ref})\big)(\lambda_w - \lambda_r) + \lambda_r,$$

$$\theta_e(\xi,\omega,u) = h(\omega)\theta_m(\xi,\omega,u).$$